Supporting Information for

Novel Nanocarriers for Silencing Anti-phagocytosis CD47 Marker in Acute Myeloid Leukemia Cells

*Eman M. Hassan[1], Shan Zou[1,2]**

[1]Metrology Research Centre, National Research Council of Canada, Ottawa, K1A 0R6, Canada;

[2]Department of Chemistry, Carleton University, 1125 Colonel By Drive, Ottawa, ON K1S 5B6, Canada

Synthesis of GO [S1]

1.0 g of flake graphite (7782-42-5, Graphene Supermarket, USA) and 1.0 g KNO_3 (P6083-500G, Milipore Sigma, USA) were added to 35 mL H_2SO_4 (58780, ACP, Canada) over ice. 4.5 g of $KMnO_4$ was added to the solution over 75 minutes with stirring. The solution was stirred for 24 h, and was then allowed to sit for another 4 days. The solution was added to 110 mL of 5 wt% H_2SO_4, followed by adding 9 mL of 30 wt% H_2O_2 in water. The solution was diluted and washed for four times by using 3 wt% H_2SO_4, 0.5 wt% H_2O_2 in H_2O, with centrifugation for 20 min at 10 000 rpm. Following the acidic washes, the precipitate was washed an additional 8 times with water. The resulting approximately 100 mL of translucent brown 'gel' was measured to have a concentration of 8 mg/mL, which was further centrifuged at 20 000 rpm for 1 h. The resulted GO material is labelled as “big-GO”.

Characterization of GO and GO conjugates

Dynamic light scattering (DLS) measurements of GO and GO conjugates were performed on the Zetasizer Nano ZS particle size analyzer (Malvern Instruments, UK) in a semi-micro polystyrene disposable cuvette (VWR, USA). Samples for DLS were diluted to 4 μg/mL in MiliQ water [2]. Measurements were performed at 25 $^{\circ}$C with 180 s of equilibration time. The measurement angle was set to 173° with 0.4 to 10 000 nm as the detectable particle range. Each sample was measured five repeat indications, with each indication being an average of eleven 10 s long runs. For small-GO and small-GO-PEG-PAMAM samples, the instrument output Z-average hydrodynamic diameter (Z-avr) values were determined by the cumulants method with the Zetasizer Software parameters set at their default values. The five indications for each sample were averaged and the mean Z-avr with corresponding standard deviations were reported. The cumulants analysis is a robust method applicable to monomodal and nearly monodisperse samples, which is less suitable for GO formulations in general. It is important to note that the intensity-weighted arithmetic-average equivalent sphere hydrodynamic diameter, which was used as the descriptor for the flake size of the GO materials [S1-S3]. With increasing complexed components in the siRNA transfection media, applicability of the cumulants analysis maybe limited with Z-avrtaking effective values not directly indicative of the size and size distribution of primary flackes. In such cases, the measurements were further evaluated suing the non-negative least squrares (NNLS) distribution analysis. A number-weighted conversion is carried out Using the Zetasizer software ver. 8.0 research, with the high resolution NNLS multimodal distribution method in the 10 nm to 6 µm range with 70 size classes (bins) distributed logarithmically over the 10 nm to 10 µm range. Samples showed bimodal average diameter distribution in the analysis range (10 nm to 6 µm), see Figure S2.

Atomic force microscopy topography imaging was carried out using the MultiMode AFM with a NanoScope V controller (Bruker Nano Surfaces Division, Santa Barbara, CA, USA), in Peak Force QNM mode. The peak force with which the tip taps the sample surface was always kept at the lowest stable imaging level of 200–400 pN. Silicon nitride ScanAsyst-Air AFM probes (Bruker AFM Probes, Camarillo, CA, USA) were used in all peak force feedback measurements. Their manufacturer specified typical tip diameter and spring constants are 2 nm and 0.4 N/m, respectively. While images of sizes of up to 20 µm x 20 µm were acquired to ensure good homogeneity without overlapping of flakes of GO and GO-conjugates, all the images used to measure the size of the flakes were 1–2 µm and 2.5–5 µm in scan size, for small-GO (or GO-conjugates) and big-GO (or GO-conjugates), respectively, acquired with 512 × 512 pixel resolution. The AFM probe cantilever was vertically oscillated at 2 kHz, at a lateral scan rate of 0.8–1.4 Hz.

The chemical properties of GO and GO conjugates were carried out by using a Fourier transform infrared (FTIR) spectrometer (Nicolet 6700, ThermoFisher) equipped with a substrate sample holder accessory (that allow measurements of GO-conjugate thin films on silicon substrates), in the range of 4000 to 400 cm^{-1} with a resolution of 4 cm^{-1}. The generation of amide groups, increased intensity of C–O and decreased intensity of C=O groups in GO, confirmed the successful formation of GO-PEG-PAMAM and GO-PEG conjugates.

Cell transfection with CD47_siRNA followed by flow cytometric measurements

CD33_siRNA, CD47_siRNA, the siRNA controls (with scrambled sequences and FITC labeled CD47_siRNA) and all other materials such as buffers for transfection were purchased from Santa Cruz Biotechnology Inc., USA. CD34_siRNA and controls were purchased form Integrated DNA Technologies (IDT), USA. Lipofectamine RNAiMAX transfection reagent was purchased from ThermoFisher, USA. PE anti human CD33, CD34 and CD47 antibodies, cell staining buffer, and human TruStain FcX™ (Fc Receptor Blocking Solution) were purchased from BioLegend (USA).

All cells were seeded at 3×10^5 in 6-well tissue culture plates. Cells were allowed to grow and reach 60-70% confluency. Then transfection-mix was prepared according to the manufacture instructions. Typically, CD47_siRNA (in the amount of 3:1 CD47_siRNA:GO or GO-conjugates) was mixed with the transfection reagent (unless otherwise stated), then each of the GO formulation was added to the transfection-mix at a final concentration of 5 μg/mL and incubated for 30 min at room temperature (21 ± 2 °C), labeled as transfection-mix-GO. Then different transfection-mix-GOs (with respective GO formulations) were added to each cell line, respectively, and allowed to incubate overnight (16–24 h). To ensure that CD47_siRNA was delivered specifically to the target cells, two controls were used; control 1 and control 2, which are scrambled sequence of the CD47_siRNA. A negative FITC conjugated CD47_siRNA was used to evaluate the uptake of the target siRNA by the cells. For CD33_siRNA and CD34_siRNA, only one control was used and transfection tests were only carried out in HL-60, NB4 and PBMC cells.

For positive control experiments, lipofectamine RNAiMAX transfection reagent was added to each cell line with CD33-siRNA, CD34_siRNA, or CD47_siRNA, according to the manufacturer instructions. Briefly, each of the siRNA and lipofectamine RNAiMAX (*e.g.,* 3:1 CD47_siRNA: lipofectamine RNAiMAX) were diluted in Opti-MEM media in separate tubes, then they were mixed in the same tube and allow to stand for 10-15 min at room temperature (21 ± 2 °C). Then the transfection mix was added to each cell line, respectively, and allowed to incubate overnight (16–24 h). Then all cells were harvested for standard antibody staining with PE anti human CD33, CD34, or CD47 antibodies to measure levels of CD33, CD34, or CD47 expression before and after transfection using flow cytometry analysis (BD-FACS Canto model 640166, SN: V0099, USA). The siRNA knockdown efficiency of CD markers of each cell lines was calculated according to the below formula:

$$\text{knockdown efficiency (\%)} = (MFI_{\text{un}} - MFI_{\text{trans}})/MFI_{\text{un}} \times 100\% \qquad \text{S(1)}$$

where MFI_{un} is the mean fluorescence intensity of un-transfected cells, MFI_{trans} is the mean fluorescence intensity of cells with added transfection-mix-GOs.

The percentage of cells undergoing apoptosis were evaluated in all cell lines, using PE Annexin V apoptosis detection kit (BD Biosciences, Canada) followed by flow cytometry analysis. All flow cytometric data was analyzed using flowJo software (10.6 version, 2019).

Cytotoxicity assay and CD47 siRNA and GO formulation ratio analysis

All cell lines mentioned were seeded in a 96 well tissue culture plate (5×10^3 cells per well) and treated with 0, 1, 5, 10, 15, and 25 µg/mL of different formulations of GO overnight at 37 °C and 5% CO_2. Then, WST-8 reagent (Cell Counting Kit 8, VistaLab Technologies, USA) was added to each well (10 µL) and incubated for 2 h at 37 °C. The optical densities of the WST-8 treated plates were measured at 460 nm using a plate reader (Multiskan™ FC photometer microplate reader, Thermo Fisher, Canada). Viability percentage was calculated as:

$$viability = \frac{OD_{sample\ n} - OD_{sample\ blank\ n}}{OD_{control} - OD_{control\ blank}} \times 100\% \qquad \text{S(2)}$$

where $OD_{sample\ n}$ is the optical denisty of the cell containing sample with *n* µg/mL GO treatments, $OD_{sample\ blank\ n}$ is the optical density of the same *n* µg/mL GO without cells present, $OD_{control}$

is the optical denisty of the untreated cells and $OD_{control\ blank}$ is the optical density of the media alone.

Small-GO-PEG-PAMAM (1 µg) was mixed with CD47 siRNA at different ratios (w/w: 1–10) and incubated at room temperature for 30 min. The complexes were then added to flat bottom 96-well plate and read at absorbance of 260 nm.

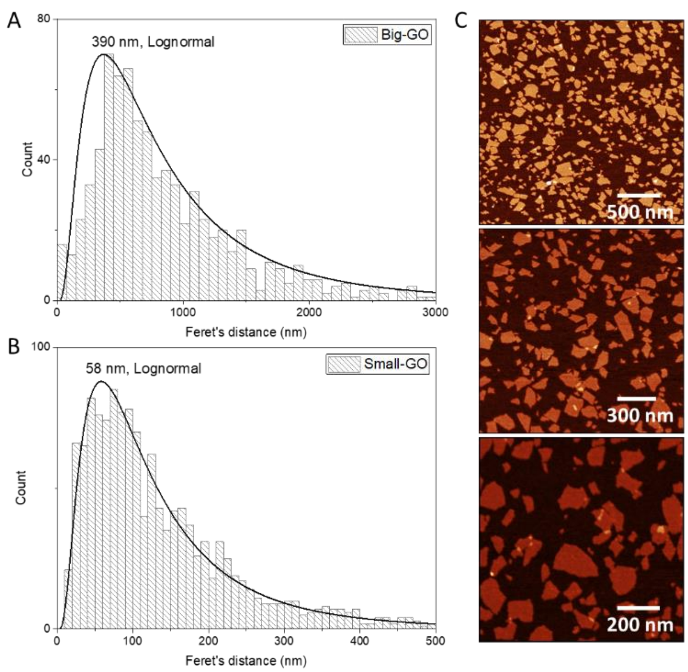

Figure S1. Size distributions of GO flakes of (A) big-GO (N=795, Mean: 945 nm, Median: 698 nm, Lognormal fit maximum: 390 nm) and (B) small-GO (N=1336, Mean: 118 nm, Median 105 nm, Lognormal fit maximum: 58 nm). (C) AFM images of small-GO with different scan sizes.

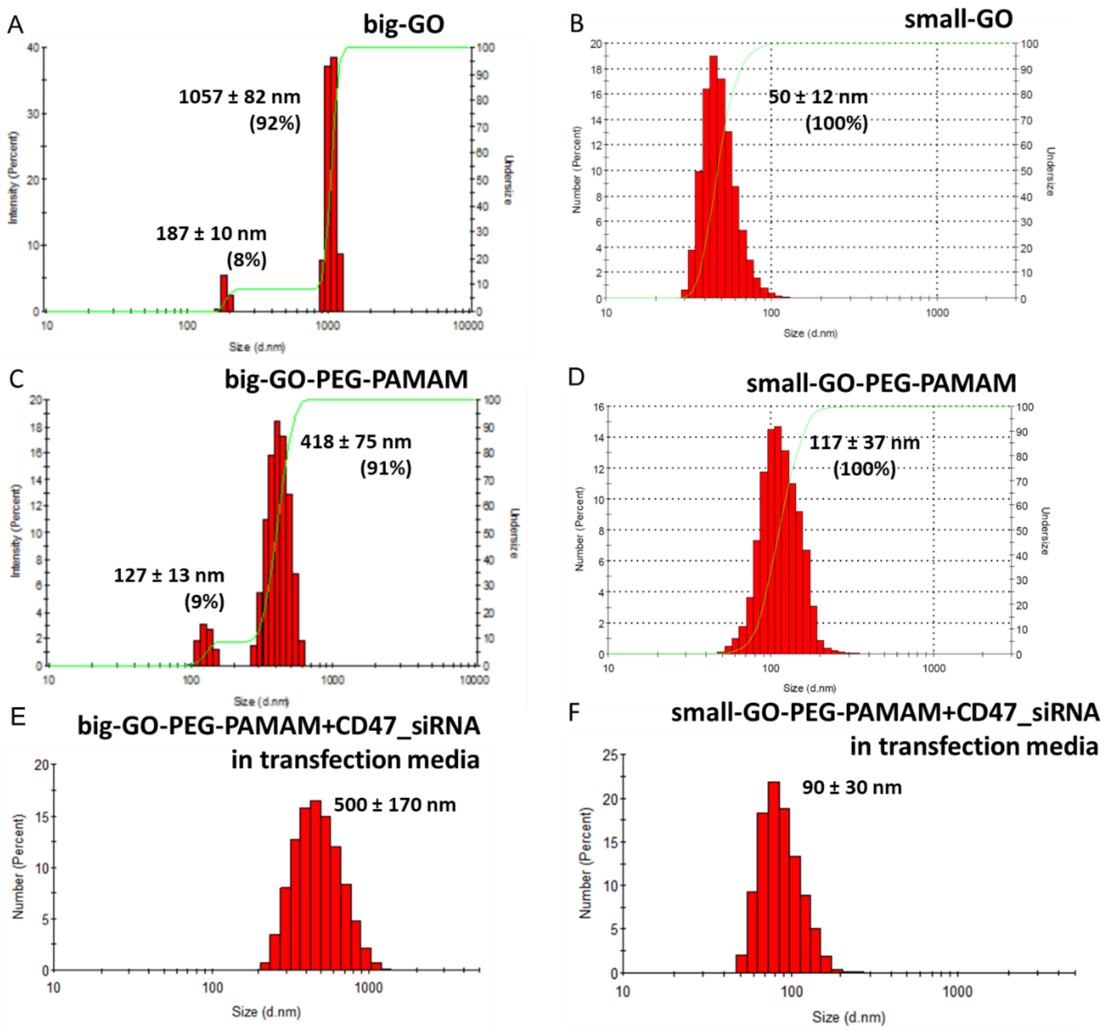

Figure S2. Size evaluation of big-GO (A), small-GO (B), big-GO-PEG-PAMAM (C), small-GO-PEG-PAMAM (D), big-GO-PEG-PAMAM with CD47_siRNA (E) and small-GO-PEG-PAMAM with CD47_siRNA (F) in transfection media by dynamic light scattering (DLS) measurements. It should be noted that the conversion from intensity weighted to number weighted plots should be paid great attention. Data process using peak suppression trick is applied to the siRNA containing samples as there are many salt, protein and sugar molecules presented in the media.

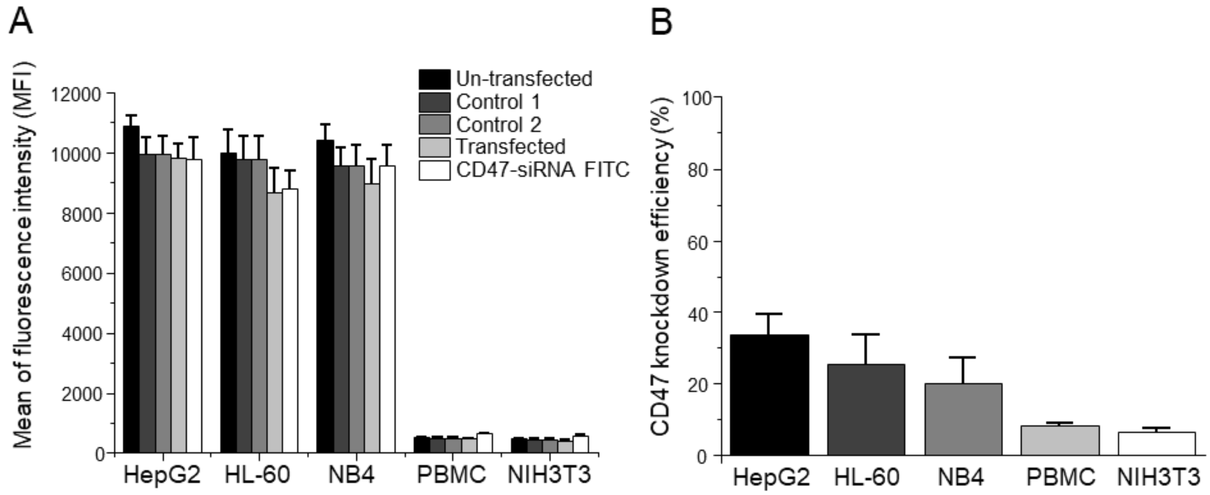

Figure S3. Knockdown efficiencies in different cancer and normal cell lines without using GO as the carrier for CD47_siRNA. (A) Mean of fluorescence intensity (MFI) of CD47 marker after transfection with CD47_siRNA, control 1, control 2, and the negative control FITC conjugated siRNA in HepG2, HL-60, NB4, and PBMC cells. MFI was measured after staining the cells with anti-CD47 antibody (PE labeled). (B) Knockdown efficiency of CD47_siRNA without using GO carrier in all cell lines used. Values in the graphs are shown as mean ± SEM of three trials of duplicate samples (n=6).

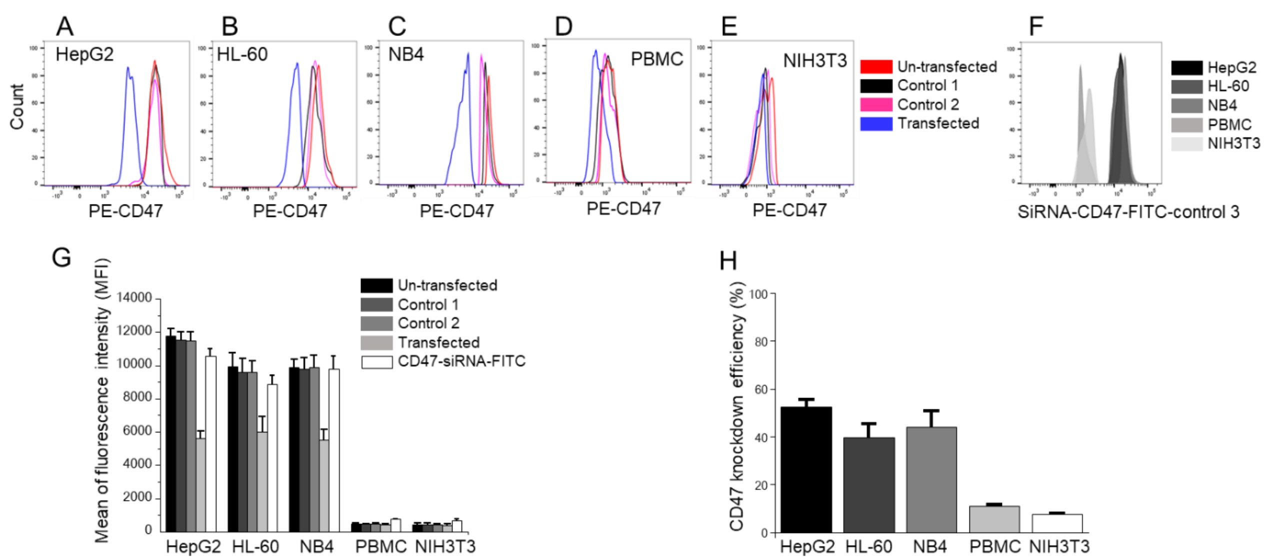

Figure S4. Flow cytometry measurements of CD47 expression levels and knockdown efficiency of CD47-siRNA in different cell lines using small-GO as carriers. (A-E) Overlay-flow cytometric histograms represent the expression level of CD47 (labeled with PE) after CD47_siRNA transfection in (A) HepG2. (B) HL-60, (C) NB4, (D) PBMC, and (E) NIH3T3. (F) Overlay-histograms of FITC labeled CD47_siRNA as negative control in all cell lines used. (G, H) Summary of MFI and calculated knockdown efficiency values of CD47_siRNA in all cell lines used. Values in the graphs are shown as mean ± SEM of three trials of duplicate samples (n=6).

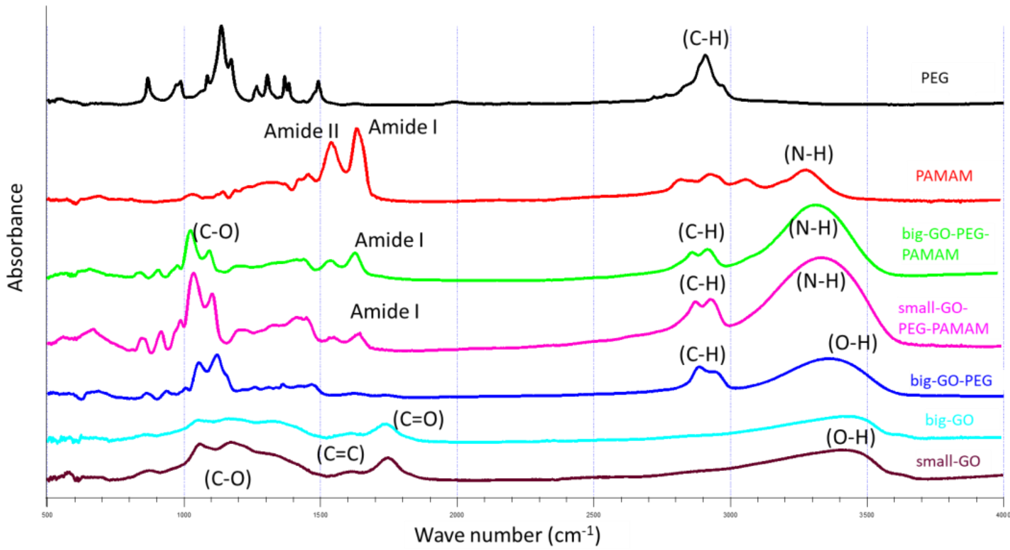

Figure S5. FT-IR spectra of GO and GO-conjugates. Functional groups such as O–H, C=O and C=C on GO react with PEG and PAMAM, with decreased absorbance intensity (or completely disappeared) on GO-conjugates; new functional groups such as amide groups and sharp C–O were evidently observed on GO conjugates.

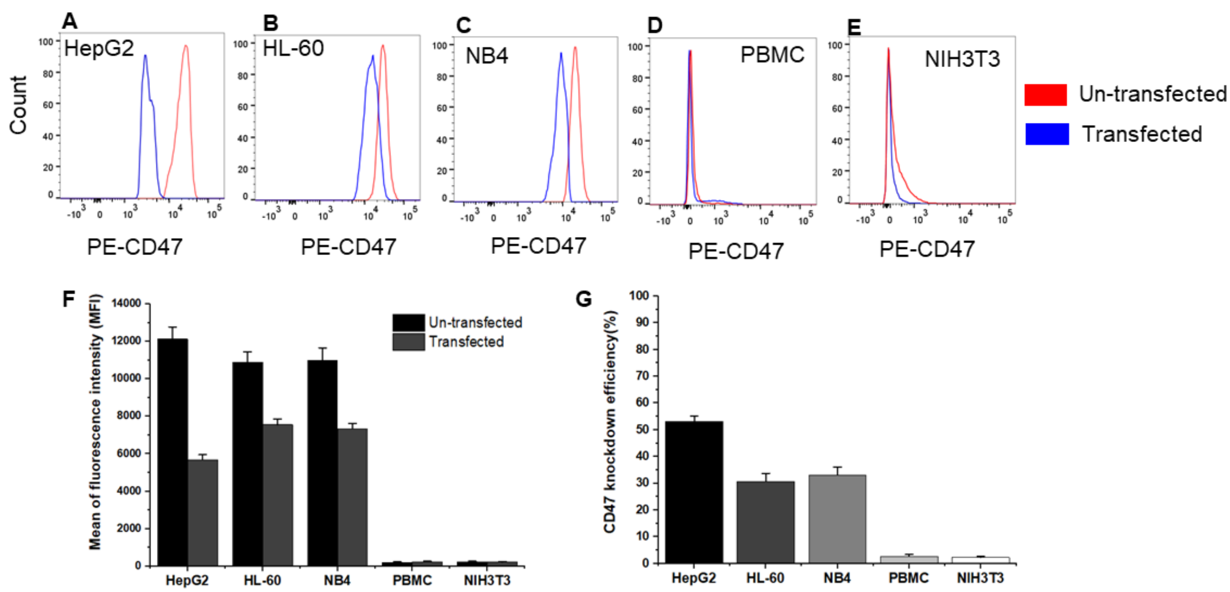

Figure S6. Flow cytometry measurements of CD47 expression levels and knockdown efficiency of CD47-siRNA in different cell lines using lipofectamine RNAiMAX as carriers. (A-E) Overlay-flow cytometric histograms represent the expression level of CD47 (labeled with PE) after CD47_siRNA transfection in (A) HepG2. (B) HL-60, (C) NB4, (D) PBMC, and (E) NIH3T3. (F, G) Summary of MFI and calculated knockdown efficiency values of CD47_siRNA in all cell lines used. Values in the graphs are shown as mean ± SEM of three trials of duplicate samples (n=6).

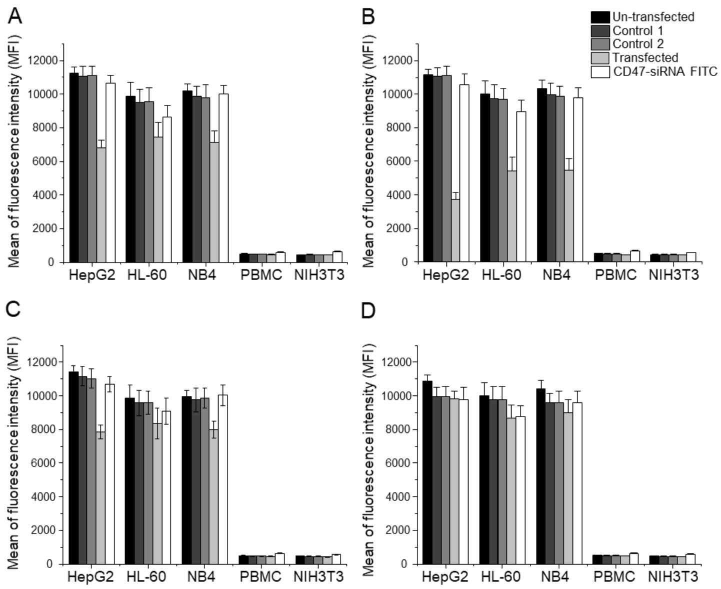

Figure S7. Mean of fluorescence intensity (MFI) of PE labeled anti-CD47 antibody in cancer and normal cells. Different GO and PAMAM formulations were used as carriers: (A) GO-PEG, (B) PAMAM 1 µg/mL. (C) PAMAM 10 µg/mL. and (D) GO-PAMAM. Values in the graphs are shown as mean ± SEM of three trials of duplicate samples (n=6).

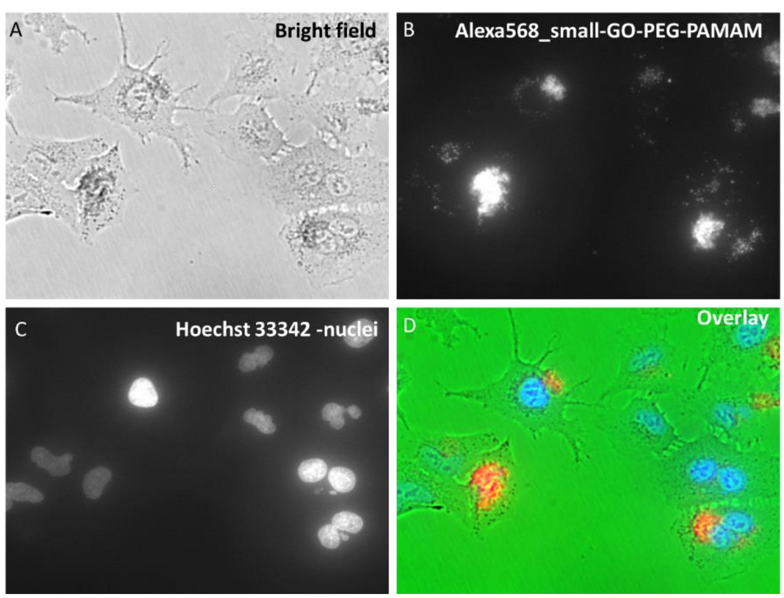

Figure S8. Uptake of small-GO-PEG-PAMAM in HepG2 cells: Bright field (A), epi-fluorescence images of Alexa 568 labeled (B), Hoechst 33342 nuclei staining (C), and overlay (D). HepG2 cells were seeded on bottom-glass culture dishes overnight, then treated with 20 µg/mL small-GO-PEG-PAMAM for 48 h, followed by washing with FluoroBrite DMEM (3×2 mL). Images were taken by using 40× objective and the size of images are 224 µm by 168 µm, using CoolSNAP camera, 1340 by 1040 pixels.

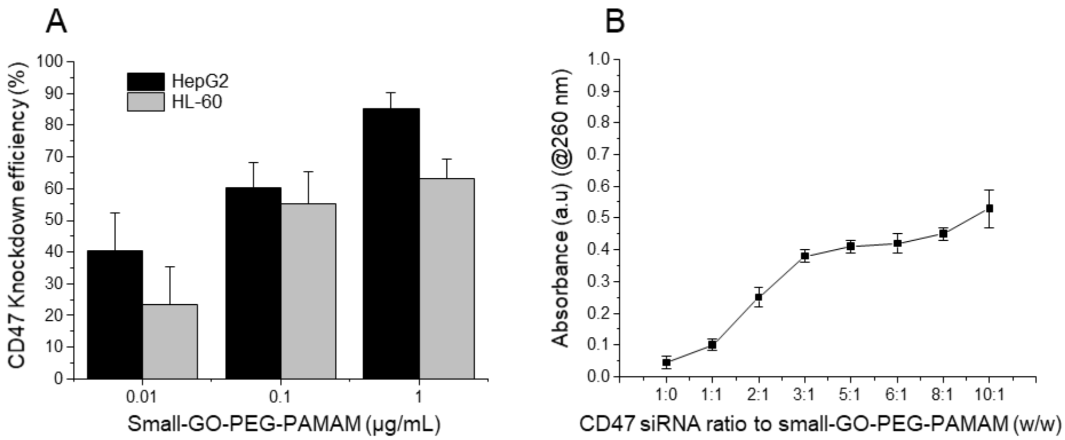

Figure S9. Knockdown efficiency CD47_siRNA in HepG2 and HL60 cells. (A) Bar graph shows the calculated CD47_siRNA knockdown efficiency using small-GO-PEG-PAMAM as carriers in HepG2 and HL-60 at concentrations of 0.01, 0.1, and 1 μg/mL. (B) Binding ratio curve of CD47_siRNA and small-GO-PEG-PAMAM. Values in the graphs are shown as mean ± SEM of three trials of duplicate samples (n=6) for (A) and three trials of triplicate samples (n=9) for (B).

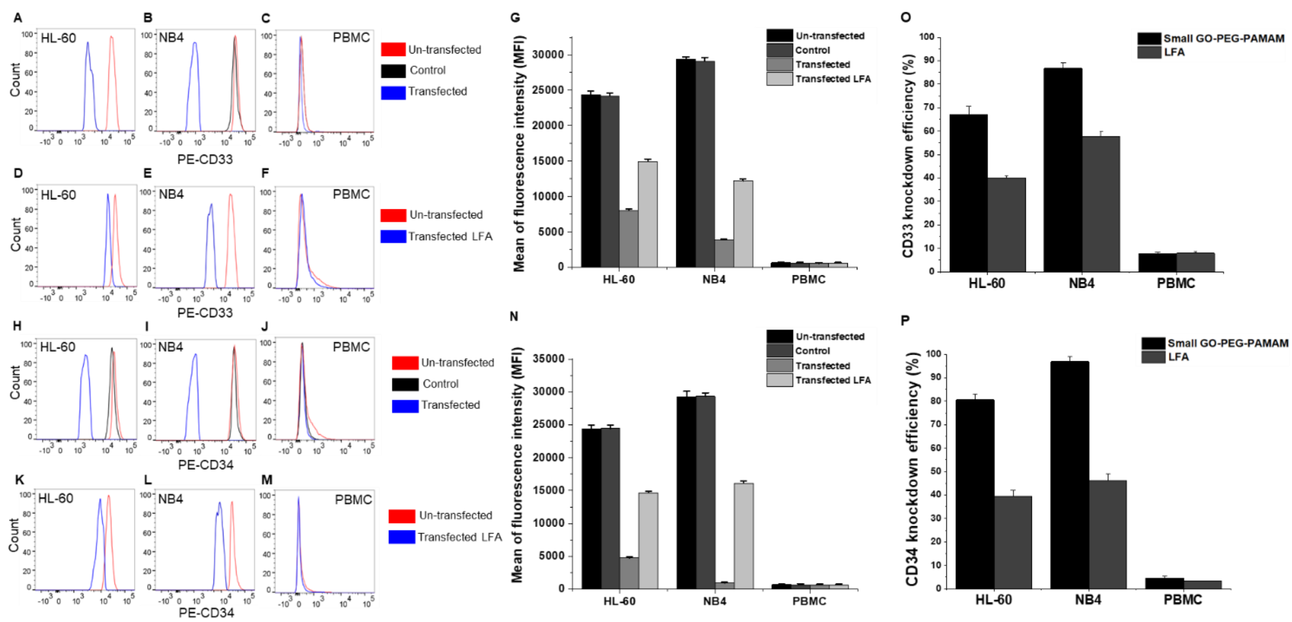

Figure S10. Flow cytometry measurements of CD33 and CD34 expression levels and knockdown efficiency of down-regulation of both markers in (A, D, H, K) HL-60, (B, E, I, L) NB4, and (C, G, J, M) PBMC using small-GO-PEG-PAMAM (A, B, H, I) and lipofectamine RNAiMAX (LFA) (D, E, K, L) as carriers. Overlay histograms of the expression levels of CD33 (A-F) and CD34 (H-M) (both are labeled with PE) after CD33_siRNA and CD34_siRNA transfection. Summary of Mean of fluorescence intensity (G, N) and calculated knockdown efficiency values (O, P) of CD33_siRNA (G, O) and CD34_siRNA (N, P) in the three cell lines used. Values in the graphs are shown as mean ± SEM of two trials of triplicate samples (n=6).

References:

S[1] V. Gies, G. Lopinski, J. Augustine, T. Cheung, O. Kodra, S. Zou, The impact of processing on the cytotoxicity of graphene oxide, Nanoscale Adv. 1 (2019) 817−826, https://doi.org/10.1039/C8NA00178B.

S[2] B.R. Coleman, T. Knight, V. Gies, Z.J. Jakubek, S. Zou, Manipulation and Quantification of Graphene Oxide Flake Size: Photoluminescence and Cytotoxicity, ACS Appl. Mater. Interfaces 9 (2017) 28911−28921, https://doi.org/10.1021/acsami.7b08585.

S[3] V. Gies, S. Zou, Systematic toxicity investigation of graphene oxide: evaluation of assay selection, cell type, exposure period and flake size, Toxicol. Res. 7 (2018) 93−101, https://doi.org/10.1039/C7TX00278E.